Article:
Ilyinskaya, E orcid.org/0000-0002-3663-9506, Mobbs, S orcid.org/0000-0003-3872-9422, Burton, R et al. (11 more authors) (2018) Globally significant CO_2 emissions from Katla, a subglacial volcano in Iceland. Geophysical Research Letters, 45 (19). pp. 10332-10341. ISSN 0094-8276

https://doi.org/10.1029/2018GL079096

Geophysical Research Letters

Supporting Information for

Globally significant CO_2 emissions from Katla, a subglacial volcano in Iceland

Evgenia Ilyinskaya[1]*, Stephen Mobbs[2], Ralph Burton[2], Mike Burton[3], Federica Pardini[3], Melissa Anne Pfeffer[4], James Lee[5], Stéphane Bauguitte[6], Barbara Brooks[2], Ioana Colfescu[2], Gudrun Nina Petersen[4], Axel Wellpott[6], Baldur Bergsson[4]

[1] School of Earth and Environment, University of Leeds, Leeds, LS2 9JT, UK
[2] National Centre for Atmospheric Science, Fairbairn House, University of Leeds, Leeds, LS2 9PH, UK
[3] School of Earth and Environmental Sciences, Williamson Building, University of Manchester, Manchester, M13 9QQ, UK
[4] Icelandic Meteorological Office, Bustadavegi 7-9, 108 Reykjavik, Iceland
[5] National Centre for Atmospheric Science, Innovation Way, University of York, York, YO10 5DQ UK
[6] Facility for Airborne Atmospheric Measurements, Cranfield University, Cranfield, UK

Contents of this file

Text S1.

1. FAAM instrumentation

The FAAM (http://www.faam.ac.uk/index.php) aircraft is a fully instrumented aircraft for atmospheric research. The most pertinent instrument here is the Fast Greenhouse Gas Analyzer (FGGA) from Los Gatos Research Inc (LGR): Model RMT-200, which samples carbon dioxide, methane, and water vapor at 1Hz. Using off-axis integrated cavity output spectroscopy technology, this instrument has a 1Hz 1-sigma precision of 1.82 ppb (methane) and 0.39 ppm (carbon dioxide). The nominal total uncertainties derived from the propagation of uncertainties of our World Meteorological Office traceable in-flight standards (WMO-NOAA-CO2-2007 and WMO-NOAA-CH4-2004A scales), and dry mole fraction correction for the influence of water vapor, are respectively 2.79 ppb and 0.432 ppm for methane and carbon dioxide(O'Shea et al., 2013).

The FAAM aircraft did not provide H_2S measurements capability during the 2016 missions. During the 2017 missions, a Teledyne model T101 H_2S monitor was deployed. The instrument operates an internal high temperature catalytic converter, for the oxidation of H_2S to SO_2, and subsequent SO_2 UV fluorescence detection. Given its sampling flowrate, the instrument response time was slow, with manufacturer stated 20 sec lag-time, and 120 sec rise/fall time (to 95%). In order to maintain adequate pressure at the instrument inlet for all altitudes, the air sample was pressurised with an off-the-shelf compressor (Senior Aerospace model MB-158E). The compressor drew sample air from the aircraft ram-air sampling pipe using a Teflon sampling line. Teflon tubing was also used for connecting the compressor outlet to the T101 instrument inlet.

With the above configuration, the T101 monitor did not appear to be sampling H_2S quantitatively, despite its odour being detected by cabin occupants during several flights. The minimum perceptible odour is 130 ppb according to the Occupational Safety and Health Administration, although some individuals can smell H_2S as low as 10 ppb.

We believe the stainless steel bellows of the inlet pressurisation compressor might be responsible for up-taking H_2S, prior to it being analysed by the T101 instrument. During recent laboratory testing of our airborne sampling configuration, we compared the T101 sampling performance of H_2S air mixtures ranging 25-300 ppb, using the metal bellows compressor, and an all-Teflon compressor (KNF Neuberger GmbH model N726FTE). Sampling through the metal bellows compressor required 620 sec rise time to 95% H_2S test concentration, whereas sampling through the all-Teflon compressor required 140 sec rise time to 95%. This result confirms that the small scale H2S volcanic plumes (tens of seconds crossing time) sampled in 2017 were unlikely to have been measured quantitatively.

This was further confirmed by post-flight analysis of pressurised 3L SilcoCan air sampling canisters (Thames-Restek Product Code 22091) collected by the FAAM aircraft whole air sampling (WAS) system. In-flight triggering of WAS sampling was directed by detection of volcanic plumes from in-situ FGGA measurements. WAS are pressurised to 40 psi using a different metal bellows compressor (Senior Aerospace model 28823-7). Although SilcoCan canisters have been demonstrated to effectively store very low levels of reactive sulphur compounds (eg 1-20 ppb H_2S, Restek Corp. Applications Note #59347A, 2005), no H_2S was detectable during post-flight analysis of WAS samples known to have been collected in sulphur rich plumes (over Icelandic geothermal plants), suggesting that metal bellows compressors do indeed uptake H_2S.

2. HYSPLIT

A backward trajectory analysis is performed through the HYSPLIT software(Stein et al., 2015) to constrain the source location of the excess CO_2. The meteorological data used in the HYSPLIT simulations is derived from a Weather Research and Forecasting (WRF; see SI section

3) simulation. This WRF simulation, with a horizontal resolution of 10 km and covering the entirety of Iceland, was in turn initialized with global 0.25 degree (~25 km) analysis data from the National Centers for Environmental Prediction Global Forecast System("GFS Products," n.d.). Here, the WRF simulation is designed to provide, and provide only, higher-resolution meteorological fields to HYSPLIT than those supplied in the underlying GFS analyses. Backward trajectories are initialized from the FAAM measurements points and run 12 hours back in time.

3. WRF: Gas source modelling and emission rate calculations

The Weather Research and Forecasting (WRF (Skamarock et al., 2008)) model is a widely used, open-source numerical weather prediction model which can be implemented at scales from tens of meters to thousands of kilometers. The model version used in this study is WRF 3.7.1; however, the approach is valid for previous and subsequent versions. The model can be compiled on a variety of operating systems (linux-based) and using a variety of compilers. The code includes a general compilation script that creates all the necessary executables. It is usually run on a parallel-computing system. The WRF Users page (www2.mmm.ucar.edu) contains links to download the code, and also links to various tutorial and learning resources.

To simulate the plume, the model was initialized with freely downloadable National Centers for Environmental Prediction Global Forecast System (NCEP GFS) 0.25° analyses (NOAA, 2017) for 18 October and 20 October 2016 and 4 October 2017. The analysis data contains all the meteorological fields necessary to initialise the model. The boundary conditions are also derived from these GFS data. The topography data (specifying the height above sea level of the terrain, in addition to the type of terrain, e.g. urban, sparsely vegetated, etc.) was derived from a high-resolution (approximately 0.7km resolution) USGS product which is part of the standard WRF package. The model domain is 550 km (east-west) × 400 km (south-north) at 400 m resolution, with 51 terrain-following vertical levels. The latter are of varying resolution, with the first and second model levels at 30 and 100 m above ground level (AGL) respectively and seven levels in the lowest 1 km AGL. The use of such a large domain was designed so that gas could spread throughout Iceland, and even over the sea, allowing for processes such as recirculation to be captured. This was particularly relevant for the 18 October 2018 case (flight B987) where gas was observed (and modelled, though in smaller concentrations) along the coast. It would be feasible, however (and if used operationally, more appropriate) to use a smaller domain concentrated on the region of interest.

Model runs were started at 06Z each day so that by local afternoon (when the flights were performed) a reasonable dissemination of gas has been accomplished. Model physics include (as standard) sophisticated representations of three-dimensional turbulence, land-surface processes, microphysics and radiation. For a detailed description of these physical schemes (and appropriate references) see (Skamarock et al., 2008). It should be stressed that the WRF model software contains all the programs and ancillary data (for example, the topography data) required to perform such a simulation. The WRF simulations used in this paper were performed on a 1024-processor machine and the simulations completed in near-real time. However, a smaller domain would require far less computing power.

3.1. Tracer method

Initial WRF model runs (results are discussed but not shown on figures in the main text) represented the gas plume as a simple tracer. These runs simply aimed to confirm that the general location of the gas sources was Katla, rather than other volcanic systems in Iceland. The plumes were simulated by introducing 33 passive (i.e., non-reacting and neutrally buoyant) tracers at 33 locations representing the positions of both active and dormant volcanoes (in addition to the 32 volcanic systems shown in Figure 1, the west flank of Katla was simulated as a separate source). Tracers were continuously released at the surface and were advected in the model at each time step. WRF has a tracer package as part of the standard distribution.

3.2. Dense gas specified mass flux (SMF)

The method developed in (Burton et al., 2017) showed how a dense gas could be modelled using WRF with minimal changes to the WRF code. A simple modification to the microphysics module of the code was introduced, to mimic the effect of swapping one molecule of oxygen (say) for one molecule of CO_2 (in the code, this is done by adding a new mixing ratio). This modification is in fact very easy to implement (requiring of the order of 30 lines of code), and further details (including relevant contact details) can be found in Burton et al. (2017). This then allows the release of a dense gas of fixed mass-mixing-ratio (units kg/kg). To find the emission rate corresponding to the mass-mixing-ratio, a simple box model is employed.

Assume that the source is located within a control volume $V = \Delta x\, \Delta y\, h$ m^3, and assume (without loss of generality) that the wind is parallel to the x-axis with speed U m/s. Here, Δx and Δy are the distance between grid points in the model (400 m) and h is the height of the lowest model level above ground (30 m). Suppose the source within the control volume emits at a rate of S kg s^{-1} (with no sinks) and the CO_2 is well mixed with volume-mixing-ratio q_v (kg m^{-3}). Then, denoting the residence time of an individual element of CO_2 within the control volume by τ (s), then

$$S = \frac{q_v V}{\tau}$$

Since the wind is parallel to the x-axis, then residence time is simply $\tau = \Delta x/U$ and so, using the definition of V,

$$S = Uhq_v\Delta y$$

Now, suppose that the control volume has density ρ_c then to convert the mixing ratio $q_v$to a mass-mixing-ratio q_m we use

$$q_m = q_v\rho_c^{-1}$$

Thus,

$$S = Uh\rho_c q_m\Delta y$$

For the calculations used in the paper, the mean wind U (calculated at each appropriate source location, at 10 m above the surface: a suitable proxy for winds in the lowest levels) was used; error bars correspond to the standard deviation in U.

Rearranging for q_m, we have from the above

$$q_m = \frac{S}{Uh\rho_c\Delta y}$$

Thus, in the WRF model, we can prescribe a fixed value for the emission rate S (kg s^{-1}) and define the mass-mixing-ratio at each integration using the modelled, simultaneous value of U (here, U is defined as above). As a consequence, the q_m potentially varies at each integration to keep S constant. For comparisons with the aircraft data, the simulated concentrations were interpolated to each recorded flight position to represent the concentration along the flight path. Spatially, the interpolation was performed in three dimensions. Temporally, the nearest (in time) tracer output file was used. Concentrations have been converted to ppm (excess above background levels). In Figure 2, the background concentration of CO_2 (402 ppm) was added to the excess CO_2 simulated by the model to allow direct comparison with the observations data.

4. Direct calculation of mass fluxes from measured concentration and wind fields

Two methods were employed, both using interpolation of the measured CO_2 concentrations and wind along the aircraft track. The first method uses a sophisticated statistical interpolation method – Inverse Distance Weighting (4.1). The second uses a physically-based dispersion model fitted to the observed concentrations (4.2).

We define C to be the measured (and interpolated in the methods described below) CO_2 concentration and C_{bg} to be the background concentration outside of the plumes (determined from measurements well away from the plumes). We also define U to be the magnitude of the vector wind averaged over the cross-section of the plume. Then the magnitude of the CO_2 flux, F, is given by

$$F = \iint_{A_p} (C - C_{bg})\, U dA \quad (1)$$

where the integral is over the cross-sectional area A_p of the plume. The two approaches described below differ in how the concentration C is interpolated in order to perform the numerical integration.

4.1. Inverse Distance Weighting Method (IDW)

Inverse Distance Weighting (IDW) is a deterministic method for interpolations from known measurement points to unknown points (in our case regular grid points over the plume cross-section). Interpolated values are calculated as the weighted average of K known values selected through the application of the k-nearest neighbors algorithm. A sensitivity analysis is performed to investigate the effects of uncertainties of both background concentration and number of nearest neighbors used for the interpolation. Both the CO_2 background concentration and the number of the nearest neighbors are set as uncertain input parameters defined as uniform distributions between a lower and an upper bound. The upper and lower values of the background concentration are calculated from the measurement points far from the CO_2 source (Katla caldera), while the number of the nearest neighbors are varied between the 1 and 5% of the total number of the measurement points used for the flux calculation. A Latin Hypercubic Sampling method is used to sample the background concentration and number of nearest neighbors distributions. We sampled 100 couples (each couple is composed of the background CO_2 concentration plus the number of nearest neighbors) and, for each couple, we performed the flux calculation (Eq.1). The other parameters required for the flux calculation are the wind speed and the width / altitude of the interpolation plane (see Table S1). Figure 3 in the main text shows the results of the interpolation for the different flights. Each figure shows the interpolated plane for a particular couple. The final flux is computed as mean value +- standard deviation of the 100 fluxes (100 couples). The final flux computed for each flight can vary up to the 25% due to the uncertainties on the background concentration and the number of nearest neighbors selected.

	Plane/cells width (km) *	Plane/cells altitude (m) *	BC (ppm) **	Wind Speed (ms^{-1}) ***
18 Oct 2016 (B987)	33 / 0.66	600 / 60	404.1 406.0	6.16
20 Oct 2016 (B989)	14 / 0.28	1230 / 123	401.2 402.5	4.05
04 Oct 2017 (C060) – western flank	9 / 0.18	1600 / 160	400.2 401.2	4.12
04 Oct 2017 (C060) – central caldera	14 / 0.28	2100 / 210	400.2 401.2	2.37

Table S1: Main parameters used for flux calculation through IDW. *Width and altitude of the interpolation plane and of the cells forming the interpolation grid. Cells have been defined by dividing the width and the altitude in 50 and 10 sections respectively. **Upper and lower limit of

the CO_2 background concentration computed using the measurement points far from Katla volcanic system. ***Mean plume speed computed from the airborne measurements

4.2. Gaussian plume approximation

Classical dispersion theory (e.g. Turner 1994) approximates concentration C in a plume in a turbulent flow by

$$C(x,y,z) = \frac{q}{2\pi\sigma_y\sigma_z U}\left[exp\left(\frac{-(y-y_0)^2}{2\sigma_y^2} - \frac{(z-h)^2}{2\sigma_z^2}\right) + exp\left(\frac{-(y-y_0)^2}{2\sigma_y^2} - \frac{(z+h)^2}{2\sigma_z^2}\right)\right] \quad (2)$$

where x, y and z define a coordinate system with source at $(0, y_0, h)$and x is positive in the downstream direction (y denotes the cross-plume direction: $y = y_0$ defines the plume axis). The source (of strength q) is at height h above ground0.. For this study we assumed that h=0 and that the plume is "terrain following" and that dispersion is otherwise unaffected by the terrain. The dispersion parameters σ_y (m) and σ_z (m) determine the extent of the plume spread in the y and z directions, respectively. U is the background wind speed.

The method of determining and was as follows. From each transect across a plume Eq. (2) was fitted to the data to determine at that height along with the value of σ_y and the peak value of the concentration. Then by fitting the peak concentrations at each aircraft transect height to Eq. (2), values of σ_z and q can be determined.

Uncertainties in the calculated plume parameters were determined from the goodness of fit. This method relies on the existence of a well-defined Gaussian plume (if this is not the case then the goodness of fit is poor and uncertainties large). Previous applications of this method by the authors(Lee et al., 2018) has shown that coherent plumes are unlikely when the wind speed is less than about $5ms^{-1}$.

The data fitting can be done by a variety of means: by bespoke code (as was used in this study), or off-the-shelf software such as Matlab (using the "gauss1" function). Uncertainties in fitted parameters can be derived from a least-squares analysis (Press et al. 2007). An alternative is to use a Monte-Carlo-type approach (Lee et al. 2018). Off-the-shelf packages such as Matlab usually provide uncertainties in their output. Once the fitted plume parameters are known the concentration field can be calculated from Eq. (2) and used in the application of Eq. (1) to calculate the mass flux. Shown below is a typical Gaussian approximation to the data on flight B989 at approximately 1 km a.s.l. (20 October 2016). Note that the background concentration has been removed prior to fitting. Here, the best fit parameters (including 95% confidence intervals) are C = (3.1, **3.9**, 4.8) PPM, and σ_y = (990, **1300**, 1615) m.

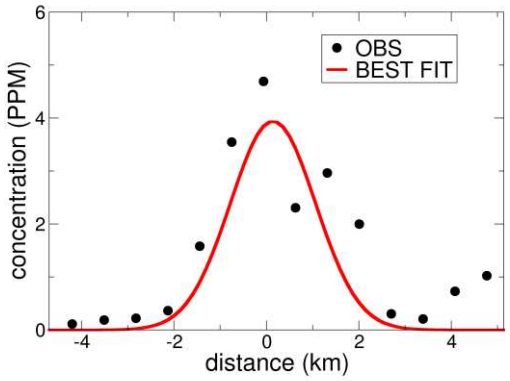

Text S1 References

Burton, R. R., Dudhia, J., Gadian, A. M., & Mobbs, S. D. (2017). The use of a numerical weather prediction model to simulate the release of a dense gas with an application to the Lake Nyos disaster of 1986. Meteorological Applications, 24(1), 43–51. https://doi.org/10.1002/met.1603

GFS Products. (n.d.). Retrieved May 7, 2018, from http://www.nco.ncep.noaa.gov/pmb/products/gfs/

Lee, J. D., Mobbs, S. D., Wellpott, A., Allen, G., Bauguitte, S. J.-B., Burton, R. R., et al. (2018). Flow rate and source reservoir identification from airborne chemical sampling of the uncontrolled Elgin platform gas release. Atmos. Meas. Tech., 11(3), 1725–1739. https://doi.org/10.5194/amt-11-1725-2018

O'Shea, S. J., Bauguitte, S. J.-B., Gallagher, M. W., Lowry, D., & Percival, C. J. (2013). Development of a cavity-enhanced absorption spectrometer for airborne measurements of CH4 and CO2. Atmos. Meas. Tech., 6(5), 1095–1109. https://doi.org/10.5194/amt-6-1095-2013

Skamarock, W., Klemp, J. B., Dudhia, J., Gill, D. O., Barker, D., & Duda, M. G. (2008). A description of the advanced research WRF version 3 (NCAR Technical Note No. NCAR/TN-475+STR). Boulder, CO: National Center for Atmospheric Research.

Stein, A. F., Draxler, R. R., Rolph, G. D., Stunder, B. J. B., Cohen, M. D., & Ngan, F. (2015). NOAA's HYSPLIT Atmospheric Transport and Dispersion Modeling System. Bulletin of the American Meteorological Society, 96(12), 2059–2077. https://doi.org/10.1175/BAMS-D-14-00110.1

Press, W. H., S. A. Teukolsky, W. T. Vetterling, and B. P. Flannery (2007). Numerical Recipes, Chapter 15, Cambridge Univ. Press, New York.

Figure S1. Full flight paths of the FAAM airborne campaigns reported in this manuscript. Volcanic systems abbreviations - ASK: Askja; BAR: Bárðarbunga; BRE Brennisteinsfjöll; ELD: Eldey; ESJ: Esjufjöll; EYJ: Eyjafjallajökull; FRE: Fremrinámar; GRN: Grímsnes; GRV: Grímsvötn; HEI: Heiðarsporðar; HEK: Hekla; HEL: Helgrindur; HEN: Hengill; HOF: Hofsjökull; HRO: Hrómundartindur; KAT: Katla; KRA : Krafla; KRI: Krýsuvík; KVE: Kverkfjöll; LAN: Langjökull; LJO: Ljósufjöll; ORA: Öræfajökull; PRE: Prestahnúkur; REY: Reykjanes; SNF: Snæfell; SNJ: Snæfellsjökull; TEY: Þeistareykir; THO: Þórðarhyrna; TIN: Tindfjallajökull; TOR: Torfajökull; TUN: Tungnafellsjökull; VES: Vestmannaeyjar

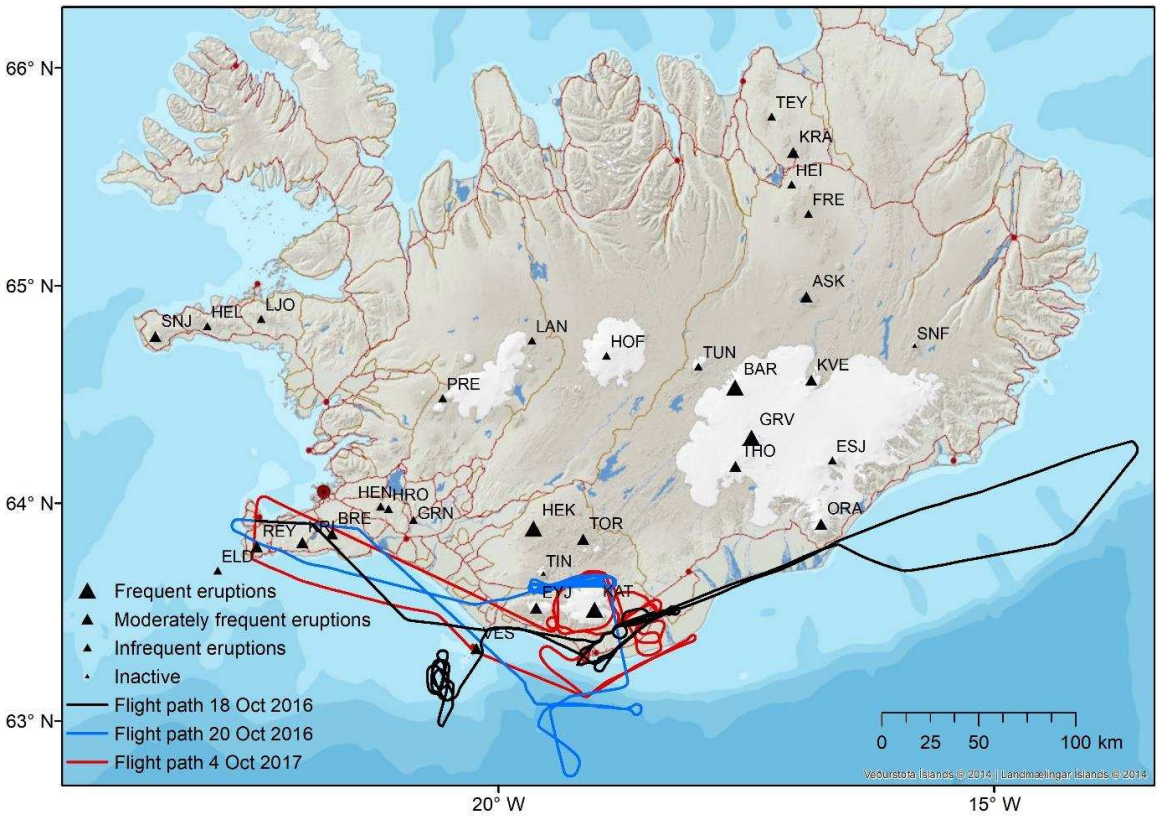

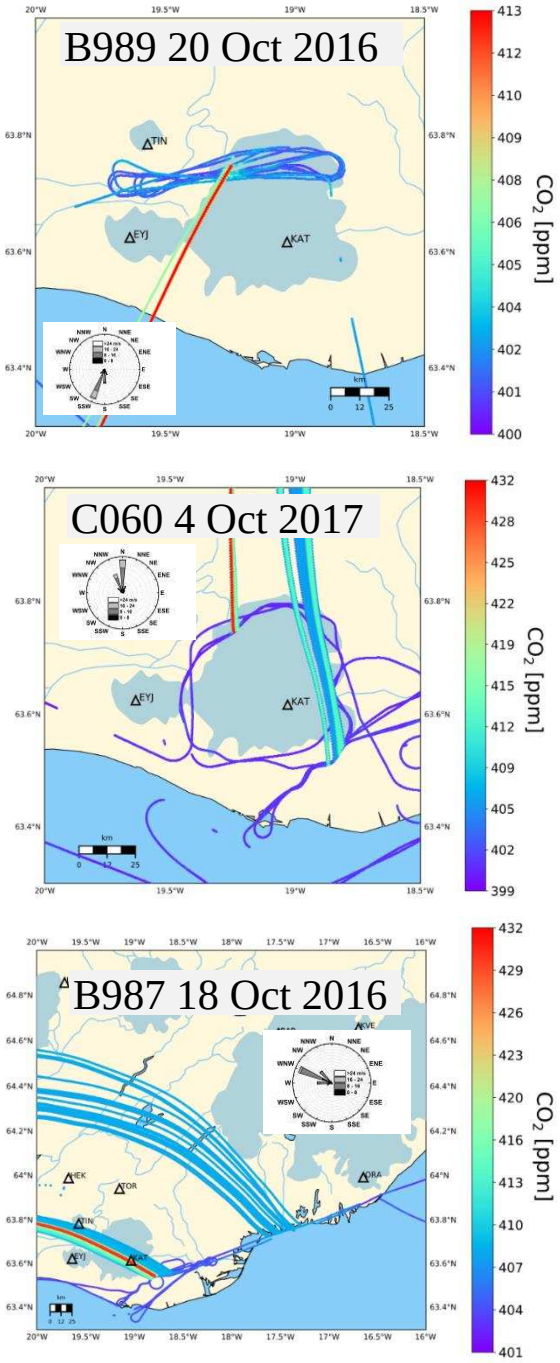

Figure S2. HYSPLIT source modelling results for enhanced CO_2 observed on flights B989 (top), C060 (middle) and B987 (bottom). Backward trajectories are initialized from the measurements points along the flight track where CO_2 peaked above the background levels, and calculated going 12 hours back in time. The trajectory lines therefore indicate where the observed air mass may have originated. All the CO_2 peaks can be traced to Katla using HYSPLIT except for the eastern CO_2 peak on flight B987. However, this peak can be traced to Katla when CO_2 is simulated as a dense gas using WRF model (see main text and Figure 2).